Supplement of Atmos. Chem. Phys., 18, 11663–11682, 2018
https://doi.org/10.5194/acp-18-11663-2018-supplement

Supplement of

Secondary organic aerosol (SOA) yields from NO_3 radical + isoprene based on nighttime aircraft power plant plume transects

Juliane L. Fry et al.

Correspondence to: Juliane L. Fry (fry@reed.edu)

In the main text, we noted a discrepancy between overall average aerosol volume estimates based on size measurements vs. AMS for the flight analyzed here (see Figure S1). We checked to see if this bias was also present in the individual plumes studied here by calculating the volume changes from the sizing instruments and the derived volume changes from the AMS+rBC mass. There is quite a bit of scatter in the volume enhancements, with most of the points falling along the same line as the data for this flight. It is unclear why the two types of volume measurements disagree more for this flight. Therefore, the bias in volume changes introduces additional uncertainty in the magnitude of the plume enhancements.

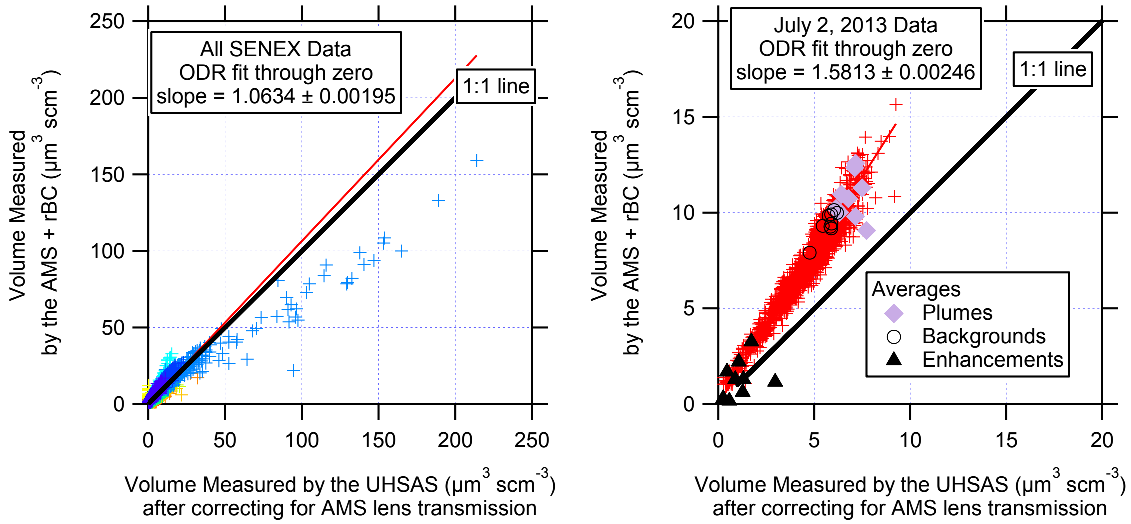

Figure S1. Aerosol volume measured using the total aerosol mass from the AMS plus refractory black carbon (rBC) and mass-weighted densities versus the aerosol volume measured by optical size with the UHSAS after correcting for AMS lens transmission. The procedure for calculating the mass-weighted density is described by Bahreini et al. [65]. On average, the measured aerosol volume from composition is roughly equal to the measured aerosol volume from size for the entire SENEX study (left hand panel) and is higher than one for the flight analyzed here (July 2, 2013, right hand panel).

Corrections for AMS UMR nitrate data and applicability to $pRONO_2$ estimation

Nitrate in the AMS is quantified in unit mass resolution mode (UMR) as the sum of the estimated NO^+ at *m/z* 30 and NO_2^+ at *m/z* 46, with a correction factor to account for the smaller ions (N^+ and HNO_3^+, mostly) produced from nitrate [83]. The default AMS UMR quantification algorithm (documented in the AMS “fragmentation table”) estimates NO^+ as the total signal at *m/z* 30 minus a small (2.2% of OA at *m/z* 29, “Org29” in AMS parlance) subtraction to account for organic interferences and an isotopic correction for naturally-occurring $^{15}N_2$ from nitrogen in air. The default UMR fragmentation table was developed for mixed ambient aerosols, in particular in urban studies, and it is the responsibility of each AMS user to correct it as needed for each study. In environments with high biogenic contributions to total OA, and/or low total nitrate concentrations, the contribution of the CH_2O^+ ion can be much larger than the default subtraction at *m/z* 30. Similarly, the $CH_2O_2^+$ ion at *m/z* 46 becomes non-negligible, and hence nitrate reported from AMS data with UMR resolution will frequently be overestimated in these situations. The poor performance of the default AMS correction is likely due to the initial focus on urban OA with high nitrate fractions when deriving those corrections [83, 84].

Here we derive a set of corrections based on an aircraft high-resolution (HR) dataset acquired with the University of Colorado HR-AMS [85] on the NASA DC-8 during the SEAC^{4}RS campaign [86]. SEAC^{4}RS took place with a strong emphasis on the SEUS 6 weeks after the SENEX flight analyzed in this manuscript. Based on an initial screening of the correlations of the CH_2O^+ and $CH_2O_2^+$ ions with UMR signals, 10 potential UMR *m/z* between *m/z* 29 and *m/z* 53 were selected as viable for deriving suitable corrections. Further analysis using three specific SEAC^{4}RS flights (RF11 on 30 Aug 30th, 2013, RF16 on Sep 11th, 2013 and RF18 on Sep 16th, 2013) that covered a wide range of OA composition with both strong biogenic contributions and fresh and aged biomass plumes showed that only four *m/z* (29, 42, 43 and 45) had good enough S/N and robust enough correlations to be used as corrections. Table S1 summarizes the correction coefficients obtained in this analysis, and Figure S2 shows the ability of matching the actual NO^+ and NO_2^+ signals (as obtained from high-resolution analysis of these flights) with the corrected UMR procedure. These corrections are applied as:

$$\text{UMR NO} = \text{Signal}(m/z30) - a_i{*}\text{Signal}(\text{Variable}_i)$$
$$\text{UMR NO}_2 = \text{Signal}(m/z\ 46) - b_i{*}\text{Signal}(\text{Variable}_i)$$

with the coefficients a_i and b_i as reported in Table S1. It should be noted that in all cases the contributions of $C^{18}O^+$ to *m/z* 30 need to be subtracted first before applying the correction (which is constrained to the organic CO_2^+ signal, measured at *m/z* 44, by the naturally-occurring isotopic ratio and assuming that OA produces $CO^+ = CO_2^+$ [87, 88]. Likewise, the contribution of $^{13}CO^+$ to Org29 needs to be subtracted first. It is hence very important for this analysis that the corrections to the AMS frag table to suitably estimate the contribution of gas phase CO_2^+ to total *UMR m/z* 44 as well as the baseline correction for *m/z* 29 be properly applied first [83]. Finally, also note that the corrections using *m/z* 29 and 43 are rather based on Org29 and Org43, which are standard AMS products that take the OA relative ionization efficiency (RIE) into account.

For the SEAC^{4}RS dataset, the corrections amounted to on average subtracting 55% from UMR *m/z* 30 and 33% from UMR *m/z* 46. Despite this large subtraction, the corrected data correlates very well with the HR AMS results, with less than 5% deviation in the regression slope between the two datasets.

Although all of the corrections in Table S1 were valid for the SEAC^{4}RS data set, for the flight analyzed here we chose Org29 to correct *m/z* 30 and *mz* 45 correction to correct *m/z* 46 because they were the closest organic signals to the UMR nitrate peaks with organic interferences and may be more valid for other field studies where different types of OA are sampled. After these UMR signals were corrected and the appropriate RIEs and CE were applied, the nitrate mass concentrations in the final data archive for the flight analyzed here were reduced by 0-0.24 μg sm^{-3}, averaging 0.11 μg sm^{-3} or 32%. The corresponding increase in

OA due to the organic interferences in the UMR nitrate had linear dependence on the reported OA mass concentrations (r^2 = 0.89) with a slope of 1.3%.

To estimate the fraction of nitrate that is organic nitrate ($pRONO_2$) the use of the NO_2^+/NO^+ ratio with an empirically determined $pRONO_2$ calibration ratio has been successfully used previously with HR-AMS data [33, 36-38, 47, 67, 89]. Figure S2 summarizes how well the ratio of the corrected UMR *m/z* 30 and 46 signals correlate with the NO_2^+ and NO^+ (and ratios) determined using HR data. As expected, there is considerable scatter at very low nitrate concentrations (which is a considerable part of the dataset, as the time series shows, since the free troposphere was sampled extensively). However, for the predicted $pRONO_2$ (which is mass-weighted), most of this scatter disappears, and for concentrations above 0.1 μg sm^{-3} of nitrate there is good agreement between the HR results and the UMR-corrected $pRONO_2$, regardless of the correction chosen. For lower concentrations the scatter is considerable larger, with the Org29 correction providing the best overall agreement. Based on the variability in this dataset for this correction (Org29), we estimate the uncertainty in $pRONO_2$ fraction apportionment using UMR to be about 30%, in addition to an estimated uncertainty for the apportionment method using HR of 20% [67]. From the comparison of UMR-corrected total nitrate to HR nitrate (not shown), we estimate an additional error of 5% for total nitrate error using these corrections.

As mentioned in the main text, the empirically determined $pRONO_2$ calibration ratio used for the flight data analyzed here was the ratio of NO_2^+/NO^+ from the ammonium nitrate calibration aerosols divided by 2.8. This factor was representative of multiple data sets analyzed by Day et al. [67]. The ammonium nitrate NO_2^+/NO^+ ratio was obtained from the two calibrations on 30 June and 7 July that bracketed the flight on 2 July, as described above. This ratio averaged 0.490. Hence, the organic nitrate NO_2^+/NO^+ ratio was estimated to be 0.175. The ratio of NO_2^+/NO^+ from the flight data was then used with the $pRONO_2$ and ammonium nitrate NO_2^+/NO^+ calibration ratios to estimate the fraction of the total corrected nitrate mass concentrations that was organic ($pRONO_2$) or inorganic (nitrate associated with ammonium or NH_4NO_3). Propagating the 30% UMR vs HR uncertainty and 20% apportionment (see above) error on top of the 34% AMS total nitrate measurement uncertainty results in ±50% uncertainties in the derived organic nitrate mass concentrations (and similar for NH_4NO_3; however it will depend on the relative contributions of $pRONO_2$ and NH_4NO_3 to total nitrate since the absolute concentration errors associated with $pRONO_2$ - NH_4NO_3 apportionment should be similar [64]).

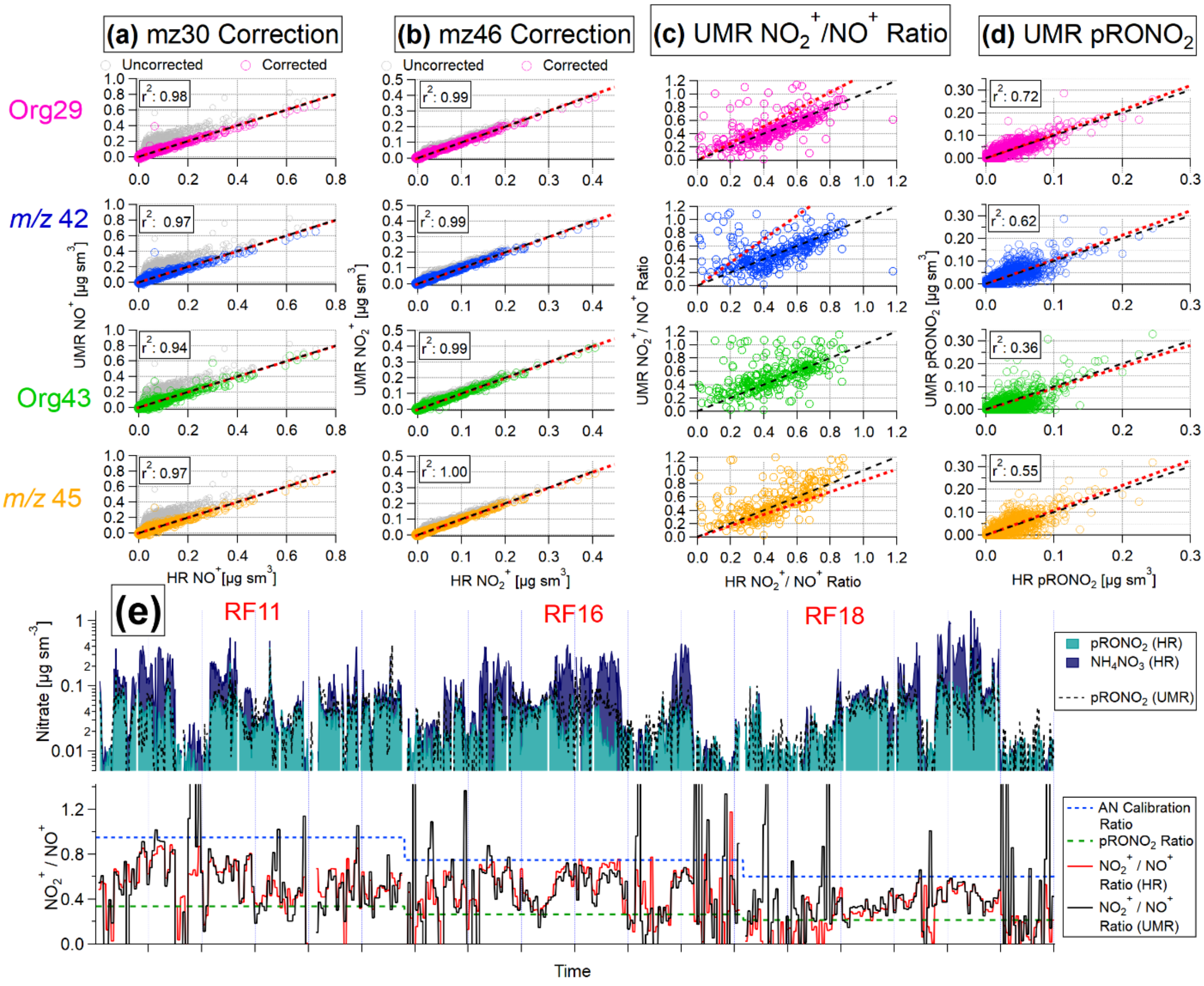

Figure S2. (a and b) Comparison of *m/z* 30 and 46 with the NO^+ and NO_2^+ signals from the high resolution analysis of the AMS data before and after applying the four different corrections listed in Table S1. The Pearson r^2 for the corrected dataset is shown as well. (c) Comparison of the NO_2^+/ NO^+ ratio obtained from HR analysis with the ratios of the corrected UMR NO and NO_2 variables (d) Comparison of the $pRONO_2$ concentrations derived using the HR and UMR NO_2^+/ NO^+ ratios using the method discussed in Day *et al* [67]. (e) Time series of the total and speciated nitrate as reported from HR analysis of the SEAC^{4}RS data [90], compared to the speciation using the Org29 correction (note the logarithmic scale). The bottom time series shows the NO_2^+/ NO^+ ratio that the speciation is based on, again for the HR and corrected UMR case.

Table S1. Coefficients used to correct *m/z* 30 and 46 to estimate total nitrate.

AMS Variable	Correction coefficient for *m/z* 30 (a_i)	Correction coefficient for *m/z* 46 (b_i)
Org29	0.215	0.037
m/z 42	0.51	0.092
Org43	0.215	0.037
m/z 45	0.72	0.127

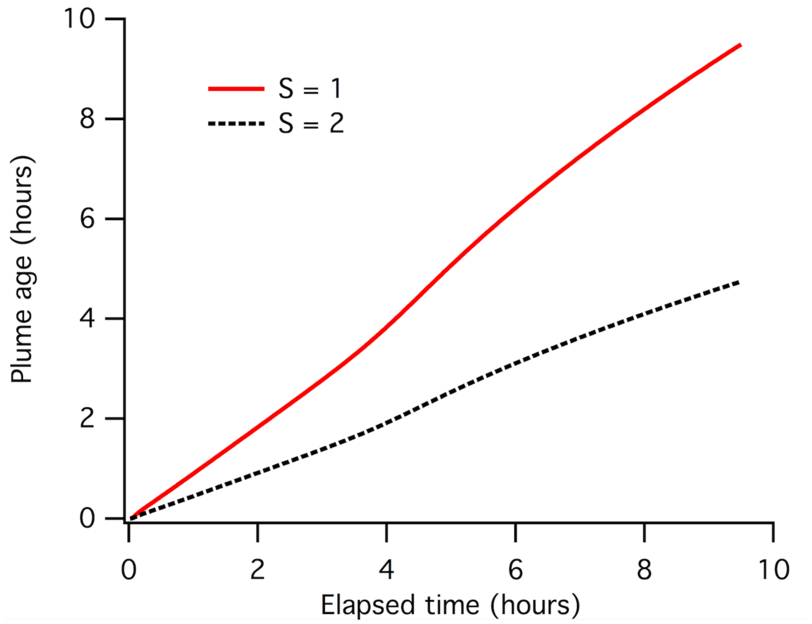

Figure S3. Calculated plume age vs. elapsed time in a box model run for a single representative night. Plume ages on the y-axis are calculated based on Equation 1 in the main text but using model NO_2 and O_3 data. Time since sunset on the x-axis is the model elapsed time (i.e., run time of the model during darkness).

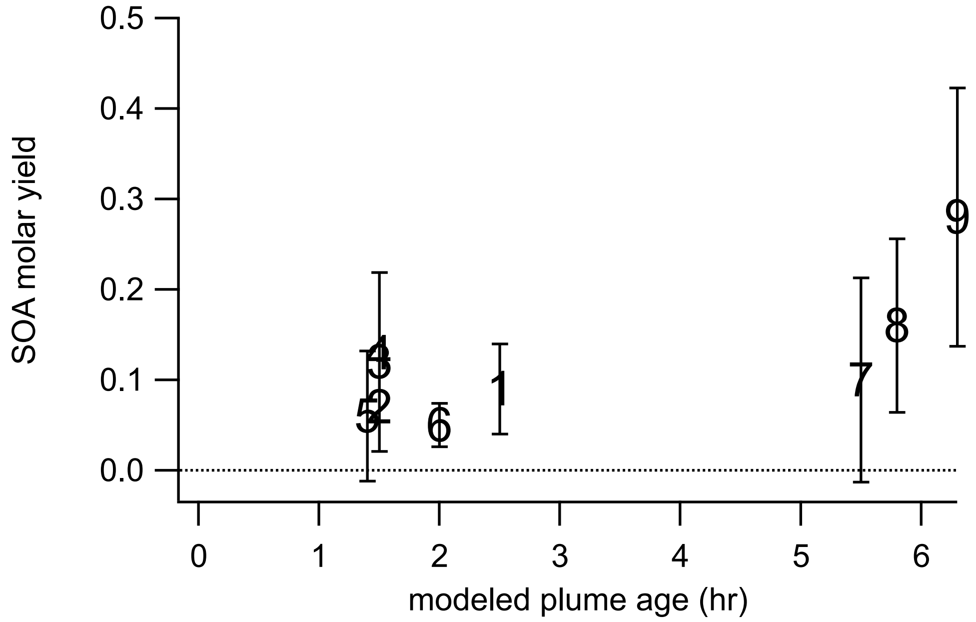

Figure S4. SOA molar yield is positively correlated with estimated plume age. This SOA molar yield is based on Eq. 3, with error bars determined by propagation of observed variability in $pRONO_2$ and isoprene, where multiple point averaging was possible. Markers correspond to plume numbers.). Based on the box model described in more detail below, the first-generation isoprene products peak at a approximately 4 hours plume age and then begin to decay.

Table S2. Peak ambient (wet) aerosol surface area during each plume used in the yield analysis (plume numbers 1 – 9), and for the two longer urban plumes transected at the end of the flight.

plume number	7/2/13 plume time (UTC)	Peak aerosol surface area ($\mu m^2\ cm^{-3}$)
1	2:18	280
2	2:20	370
3	2:21	470
4	3:03	340
5	3:55	800
6	4:34	470
7	4:37	370
8	4:39	420
9	5:04	490
Urban plume	5:36	340
Urban plume	6:37	300

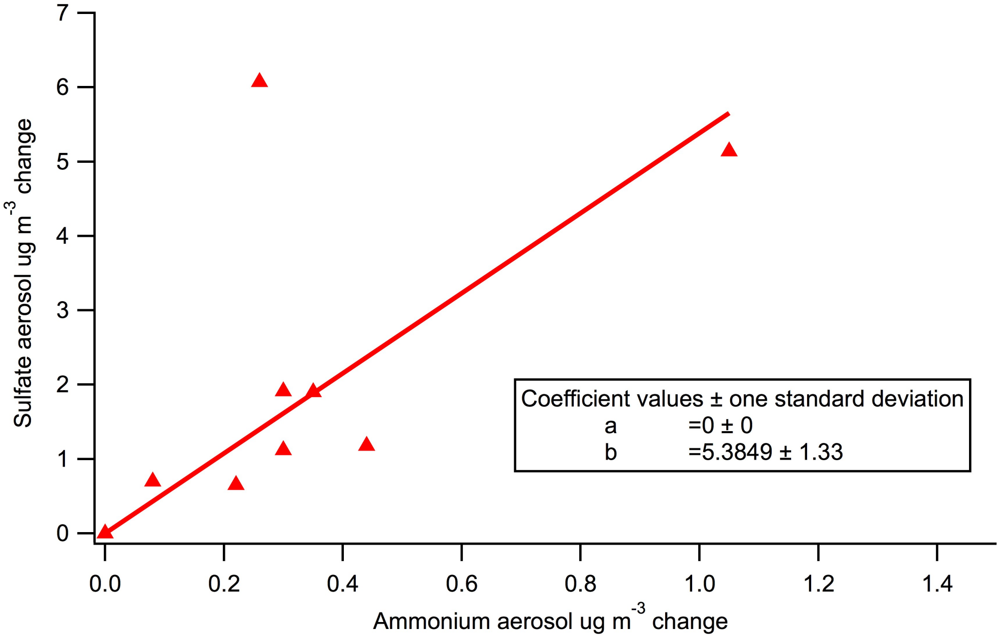

Figure S5. In-plume change in sulfate mass concentration vs. change in ammonium aerosol mass concentration is generally well correlated, with a slope of 5.4. The masses of the cations and anions would give an ion balance for pure $(NH_4)_2SO_4$ of $MW(SO_4)/(2 \times MW(NH_4)) = 2.7$, and for $(NH_4)HSO_4$ of $MW(SO_4)/(MW(NH_4)) = 5.4$. Hence, this slope provides support for a mix of these two ammonium sulfate salts, with sometimes exclusively $(NH_4)HSO_4$. This is consistent with incomplete neutralization of the sulfate mass by ammonium. The one clear outlier (sulfate increase of 6 μg m^{-3} for Plume #5) suggests excess sulfate, rendering ammonium or other inorganic nitrate formation even less likely. Points with ammonium aerosol below 0.1 μg m^{-3} are within the variability of that measurement; their omission does not change the slope.

Additional AMS and auxiliary data from plumes

Table S3. Additional information for the list of plumes used in this NO_3 + isoprene SOA yield analysis, for which key yield-related data is presented in Table 1. For each plume, the delta-values listed indicate the difference between in-plume and outside-plume background in average observed concentration. After each plume number, the numbers of points averaged for isoprene and AMS, respectively, are listed. Plume numbers annotated with * indicate brief plumes for which only single-point measurements of in-plume aerosol composition were possible.

plume number [#isop/#AMS]	**7/2/13 plume time (UTC)**	**ΔORG_{aero} ($\mu g\ m^{-3}$)**	**$\Delta NH_{4,aero}$ ($\mu g\ m^{-3}$)**	**$\Delta SO_{4,aero}$ ($\mu g\ m^{-3}$)**	**Temp (C)**	**%RH**	**Isop:MT Mole Ratio**
Typical variability ($\mu g\ m^{-3}$):		0.75	0.1	0.5			
1 [2/3]	2:18	0.35	0	0	23.6	66.5	36.5
2 [*]	2:20	0.89	0.3	1.91	23.6	65	71.4
3 [4/5]	2:21	1.25	1.05	5.14	23.6	65.2	16.6
4 [*]	3:03	0.16	0.08	0.7	21.2	68.1	50.6
5 [3/4]	3:55	0.32	0.26	6.07	21.9	65.5	34.2
6 [2/2]	4:34	0.57	0.3	1.12	19.9	74.6	17.3
7 [5/6]	4:37	1.05	0.22	0.65	19.7	76.2	14.2
8 [2/3]	4:39	1.26	0.44	1.18	18.3	82.2	11.0
9 [7/8]	5:04	1.45	0.35	1.9	17.2	84.8	17.8

Box model calculations

Box model simulations were performed using the Dynamically Simple Model of Atmospheric Chemical Complexity (DSMACC, http://wiki.seas.harvard.edu/geos-chem/index.php/DSMACC_chemical_box_model), containing the Master Chemical Mechanism v3.3.1 chemistry scheme (http://mcm.leeds.ac.uk/MCM/). The model approach is similar to that described in detail in Edwards et al. 2017, and the accompanying supplement, with the model run over a 9.5 hour night to simulate the nocturnal residual layer. For the nocturnal simulation used in this work (for both the plume lifetime calculation and the peroxy radical lifetime analysis in Sect. 4.3) the model was initialized with concentrations of the constraining species representative of the SENEX observations (Table S4). As the model is simulating power plant plume evolution from point of emission, a starting NO mixing ratio of 10 ppb was used to constrain NO_x, and the chemistry scheme was subsequently allowed to partition the reactive nitrogen. The top panels in Figure S7 show the evolution of key species during this nocturnal simulation.

Table S4: Species constrained (MCM v3.3.1 names) during model simulations and constraining values. Constraint column indicates if species concentrations were held at the constrained value throughout the simulation (Fixed) or allowed to vary after initialization (Initial).

Species	Mixing ratio	Units	Constraint
NO	9.28	ppb	Initial
O3	55.72	ppb	Initial
CO	134.00	ppb	Fixed
CH4	1920.00	ppb	Fixed
C5H8	2606.80	ppt	Initial
APINENE	38.87	ppt	Initial
BPINENE	195.50	ppt	Initial
LIMONENE	12.42	ppt	Initial
MACR	454.13	ppt	Initial
MVK	1006.00	ppt	Initial
IC4H10	47.00	ppt	Fixed
NC4H10	128.00	ppt	Fixed
C2H6	1199.00	ppt	Fixed
C2H4	117.00	ppt	Fixed
C2H2	145.00	ppt	Fixed
NC6H14	20.00	ppt	Fixed
IC5H12	120.00	ppt	Fixed
NC5H12	76.00	ppt	Fixed
C3H8	344.00	ppt	Fixed
C3H6	26.00	ppt	Fixed
CH3COCH3	2556.00	ppt	Fixed
BENZENE	35.90	ppt	Fixed
C2H5OH	2239.00	ppt	Fixed
MEK	309.00	ppt	Fixed
CH3OH	5560.00	ppt	Fixed

The daytime simulation used for comparison in Sect. 4.3 of the main manuscript (lower panels of Figure S7) uses the same initialization as the nocturnal simulation; with the only difference being the model is run during the daytime. Photolysis rates are calculated using TUV (https://www2.acom.ucar.edu/modeling/tropospheric-ultraviolet-and-visible-tuv-radiation-model). The daytime simulation does not accurately simulate daytime mixing ratios of species such as O_3 representative of SENEX observations. However, the intent of this simulation is to compare model daytime peroxy radical fate and lifetime with the nocturnal simulation. The presence of intense convective mixing in the daytime planetary boundary layer of the Southeast US makes accurately modeling these concentrations difficult with a zero dimensional model.

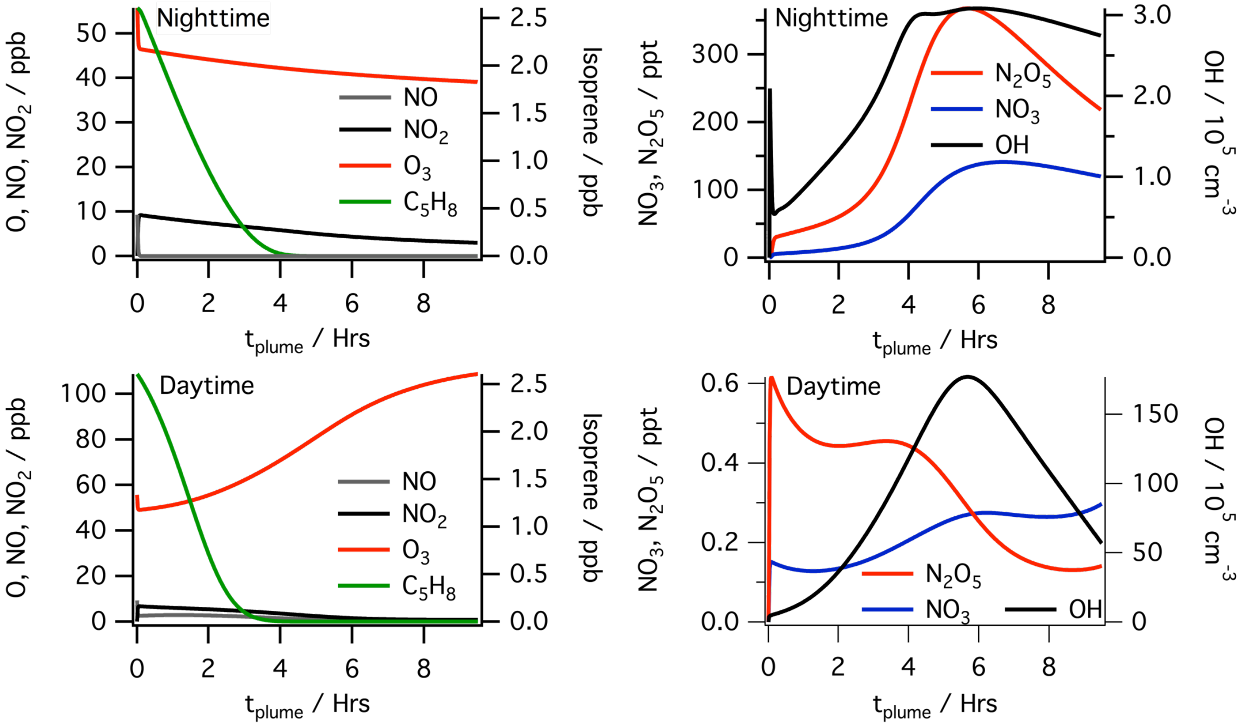

Fig. S6. Model calculated NO, NO_2, O_3, and isoprene (left) and NO_3, N_2O_5 and OH (right for the nocturnal (top) and daytime (bottom) simulations shown in Sect. 4.3.

Additional considerations investigated via RO_2 fate box modeling

Based on the potentially larger than previously estimated contribution of RO_2+RO_2 reactions at night, we considered a related possible source of a high bias in the determined SOA yields. If NO_3 reaction with the major daytime isoprene oxidation products MVK and/or MACR produces RO_2 radicals that can cross-react with NO_3 + isoprene products to produce condensable products, this would be a mechanism of recruiting isoprene-derived organic mass into the aerosol, but that original isoprene oxidation would not be counted in the denominator of the yield calculation, since its interaction with NO_3 began as MACR or MVK. In the box model, substantial MVK and MACR are available in the plume at nighttime, but only MACR reacts with NO_3, and a maximum fraction of one-quarter of MVK+MACR losses go to reaction with NO_3 overnight (see Figure S8). In addition, in our power plant plume observations, MVK+MACR are not observed to be appreciably depleted by the large NO_3 injection, further suggesting that this chemistry is not a substantial additional source of SOA (see Figure S9).

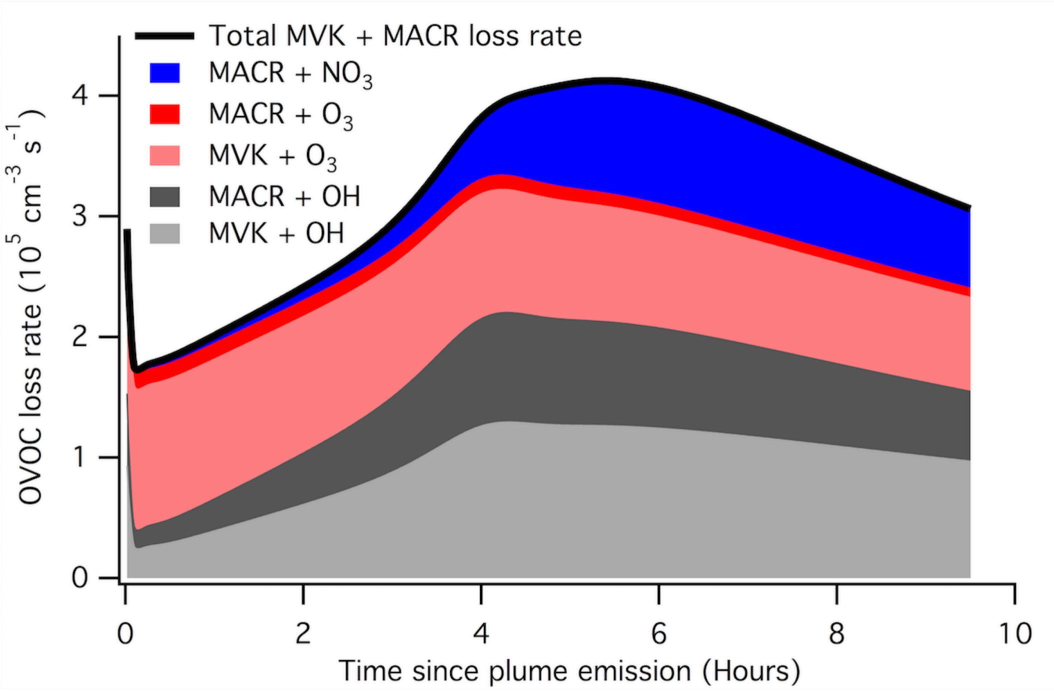

Figure S7. Calculated (via MCM) loss rate contributions for the daytime isoprene products methyl vinyl ketone (MVK) and methacrolein (MACR) in the simulated nighttime plume used in the text. Only MACR reacts with NO_3, and the contribution of this process to total losses (green stack) is relatively minor.

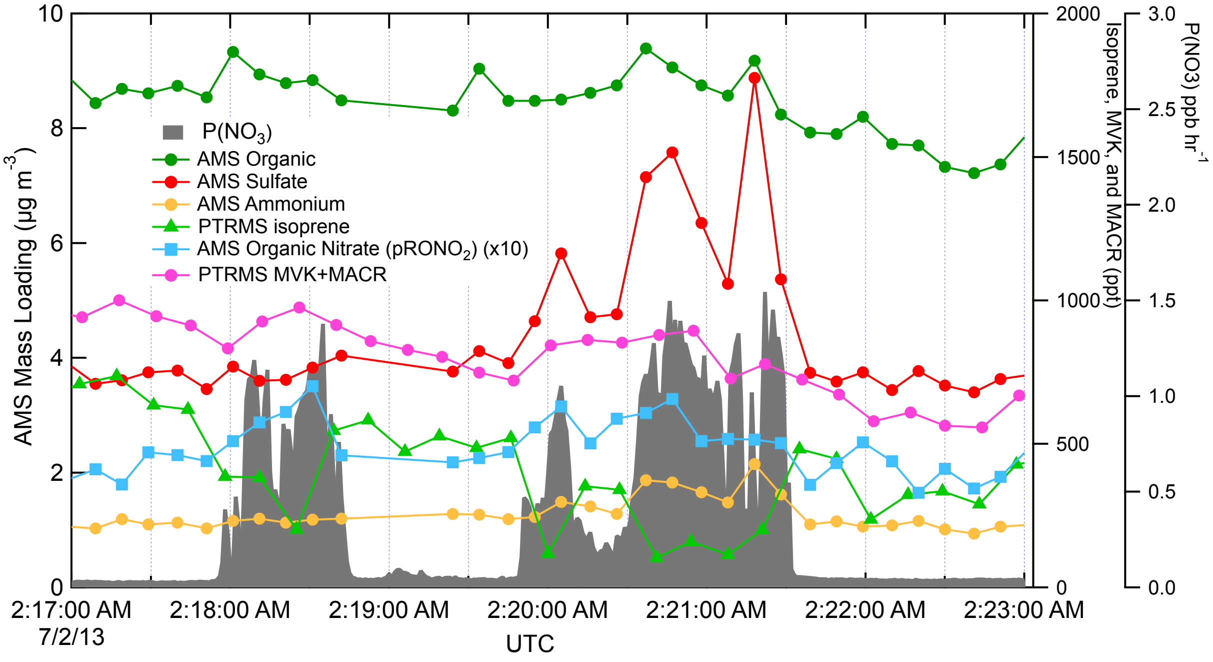

Figure S8. MVK and MACR are not titrated on the timescale of these yield estimates in power plant plumes.